Modelling and control of a SCARA robot using quantitative feedback theory

Amir-A Amiri-M[1*], **M R Gharib**[2], **M Moavenian**[2], and **K Torabi Z**[1]
[1]Department of Mechanical Engineering, University of Kashan, Kashan, Iran
[2]Department of Mechanical Engineering, Ferdowsi University of Mashhad, Mashhad, Iran

The manuscript was received on 3 January 2009 and was accepted after revision for publication on 15 June 2009.

DOI: 10.1243/09596518JSCE733

Abstract: In this paper, a practical method to design a robust controller for a SCARA robot using quantitative feedback theory (QFT) is proposed. The models used to describe robots contain uncertainties that are the result of insufficient knowledge on the dynamics of the robot, external disturbances, pay load changes, and friction, etc. Thus, the application of robust control methods to create the precise control of robots is of considerable interest. This paper considers a robot arm manipulator, a system whose models contain non-linear coupled transfer functions. In the first step of applying the QFT technique the non-linear plant is converted into a family of linear uncertain plants. This is achieved using a fixed-point theorem and then suitable disturbance rejection bounds are found. A robust controller is designed for the tracking problem. Non-linear simulations on the tracking problem for a three-dimension elliptical path are performed and the results highlight the success of the designed controllers and pre-filters. The presented results indicate that applying the proposed technique successfully overcomes the obstacles to robust control of non-linear SCARA robots.

Keywords: SCARA, robust control, linearization, QFT

1 INTRODUCTION

SCARA robots are widely used in assembly manufacturing processes. The robot is a horizontally articulated manipulator with a vertical joint at the wrist end. The link is very stiff in the vertical direction but is relatively compliant laterally. This feature is convenient for a variety of assembly tasks. Potential problems arise mainly due to the positioning errors in assembly. Adaptive and model-based controls are two of the most popular control strategies used to control robotic systems. These control schemes cannot overcome the structure uncertainties of a robotic system [**1**]. Dynamic models of robot manipulators consist of highly non-linear coupled second-order differential equations. Linear time-invariant control laws which utilize linear models of robot manipulator dynamics are often used for industrial robot manipulators because of the simplicity of the control algorithms. However, non-linearity and parameter variations in real systems prevents, ordinary linear time-invariant control schemes achieving a satisfactory control performance. Linearization techniques for the robust control of robot manipulators with uncertainty have been the subject of many research studies. For example as referenced in [**2**], Kawabata *et al.* (1993) and Takayanagi *et al.* (1993) studied robust position controllers for a two-link manipulator. Tern *et al.* [**3**] presented a dynamic modelling and linearization technique for a SCARA robot.

There are many practical systems that have high uncertainty levels in their open-loop transfer functions which makes it very difficult to create suitable stability margins and good performance in command following problems for a closed-loop system. Therefore, a single fixed controller in such systems is found among the 'robust control' family.

Quantitative feedback theory (QFT) is a robust feedback control-system design technique which allows the direct design to closed-loop robust performance and stability specifications [**4–8**].

*Corresponding author: Mechanical Engineering Department, Ferdowsi University of Mashhad, No.153, 23 Naserkhosro Street, Mashhad, Khorasan Razavi, Iran.
email: amirali1211982@yahoo.com*

Many of the techniques applied to the 'robust control' family such as H_∞ design are based on the magnitude of a transfer function in the frequency domain, QFT not only uses this transfer function approach but also takes into account phase information in the design process. The unique feature of QFT is that the performance specifications are expressed as bounds on the frequency-domain response. Meeting these bounds implies a corresponding approximate closed-loop realization of the time-domain response bounds for a given class of inputs and for all uncertainty levels in a given compact set.

Consider the feedback system shown in Fig. 1. This system has a two-degree-of-freedom structure (consider controller G(s) and prefilter F(s)). In this diagram P(s) is uncertain plant belongs to a set $P(s) \in \{P(s, \varphi);\ \varphi \in \Phi\}$ where here φ is the vector of uncertain parameters, which takes the values in Φ. G(s) is the fixed structure feedback controller and F(s) is the prefilter, and D(s) is the disturbance at the plant output.

For parametric uncertain systems plant templates must be generated prior to the QFT design (at a fixed frequency, the plant's frequency response set is called a template). Given the plant templates, QFT converts the closed-loop magnitude specifications into magnitude constraints on a nominal open-loop function (these are called QFT bounds). A nominal open-loop function is then designed to simultaneously satisfy its constraints as well as to achieve nominal closed-loop stability. In a two-degree-of-freedom design, a pre-filter is designed after the loop is closed (i.e. after the controller has been designed) [**8**].

2 SCARA ROBOT

2.1 Link matrix

The link matrix shows the position and direction of the robot, with respect to a base coordinate system.

$$\mathbf{T}_{\text{base}}^{\text{tool}} = \begin{pmatrix} & \boldsymbol{R} & & \boldsymbol{P} \\ 0 & 0 & 0 & 1 \end{pmatrix} \tag{1}$$

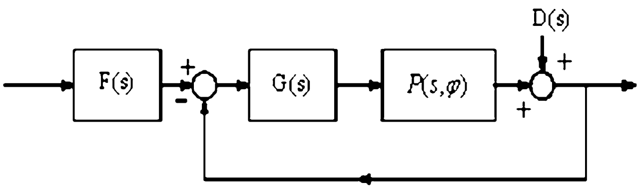

Fig. 1 Two-degree-of-freedom feedback system

where $\boldsymbol{P}$ is a vector of position and $\boldsymbol{R}$ is a vector of direction for the robot.

The shaping space of the robot has six dimensions because every robot position can be found in terms of the coordinates (P_x, P_y, P_z) and the direction characteristics of yaw, pitch, and roll. The reversed kinematics problem can be considered as: for each $\boldsymbol{P}$ and $\boldsymbol{R}$ for the robot, find the space variation value to satisfy equation (1).

If q_n is the roll angle of the robot, then the tool forming vector, $\boldsymbol{W}$ in R^6 can be written as

$$\boldsymbol{W} \equiv \begin{pmatrix} \boldsymbol{W}^1 \\ \boldsymbol{W}^2 \end{pmatrix} \doteq \begin{bmatrix} \boldsymbol{P} \\ (\exp(q_n/\pi) r^3) \end{bmatrix} \tag{2}$$

For a SCARA robot, the tool forming vector can be written as

$$\boldsymbol{W} = [P_x, P_y, P_z, 0, 0, -\exp(q_4/\pi)]^{\mathrm{T}} \tag{3}$$

2.2 Inverse kinematics for a SCARA robot

Figure 2 shows a model of a SCARA robot created using SolidWorks, and Fig. 3 illustrates the inverse kinematics chart for a SCARA robot [**9**].

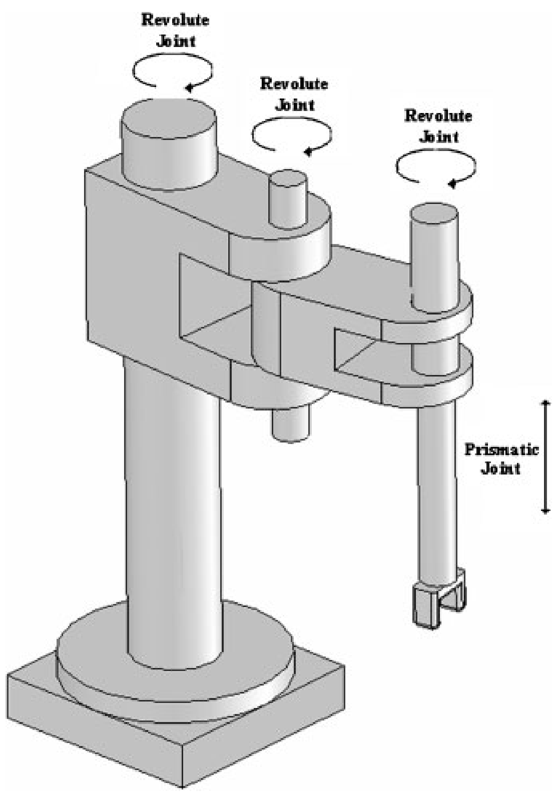

Fig. 2 The SCARA robot

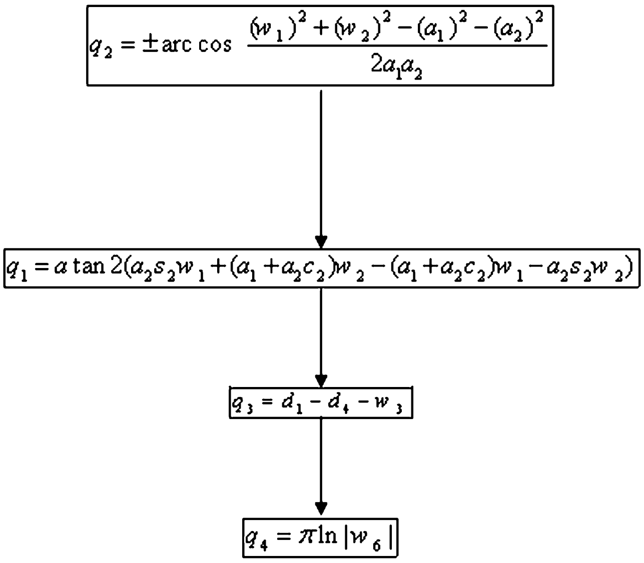

Fig. 3 Inverse kinematic chart for a SCARA robot (s_i and c_i are $\sin q_i$ and $\cos q_i$ respectively

2.3 Continuous motion

If the speed of each joint can be controlled individually, the robot can possess continuous motion in all directions. For problems where the inverse kinematics can be obtained analytically, the speed of each joint can be calculated and its derivative with respect to time can be obtained. Using the coordinate system shown in Fig. 4 the following equations can be written

$$\dot{q}_2 = \pm \frac{2(w_1\dot{w}_1 + w_2\dot{w}_2)}{\sqrt{2a_1a_2{}^2 - \left[(w_1)^2 + (w_2)^2 - (a_1)^2 - (a_2)^2\right]^2}} \tag{4}$$

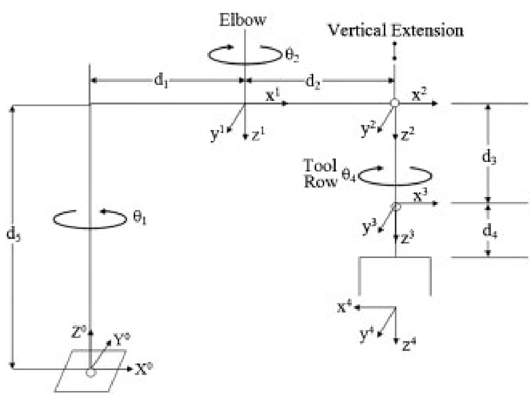

Fig. 4 Link coordinate diagram of the SCARA robot

$$\dot{b}_1 = (a_1 + a_2C_2)\dot{w}_1 - a_2S_2\dot{w}_2 - a_2(S_2w_1 + C_2w_2)\dot{q}_2$$
$$\dot{b}_2 = (a_1 + a_2C_2)\dot{w}_2 + a_2S_2\dot{w}_1 + a_2(C_2w_1 - S_2w_2)\dot{q}_2 \tag{5}$$

$$\dot{q}_1 = \frac{b_1\dot{b}_2 - b_2\dot{b}_1}{(b_1)^2 + (b_2)^2} \tag{6}$$

$$\dot{q}_3 = -\dot{w}_3 \tag{7}$$

$$\dot{q}_4 = \frac{\pi\dot{w}_6}{w_6} \tag{8}$$

2.4 Dynamics of the SCARA robot

When the Newton–Euler equations are evaluated symbolically for any manipulator, they yield a dynamic equation which can be written in the form [**10**, **11**]

$$\mathbf{D}(q)\ddot{q} + \boldsymbol{C}(q, \dot{q}) + \boldsymbol{G}(q) = \tau \tag{9}$$

where $\mathbf{D}(q)$ is the $n \times n$ mass matrix of the manipulator $\boldsymbol{C}(q, \dot{q})$ is an $n \times 1$ vector of centrifugal and coriolis terms, and $\boldsymbol{G}(q)$ is an $\mathrm{n} \times 1$ vector of gravity terms.

2.5 System linearization

In the QFT method, the non-linear plant is converted into a family of linear and uncertain processes. Two techniques have been reported in the literature for this conversion: the linear time-invariant equivalence (LTIE) of non-linear plants, and the non-linear equivalence disturbance attenuation technique [**12**]. In this paper the LTIE method is used. Taghirad and Afshar [**13**] and Gharib *et al.* [**14**] have proposed a linearization technique, which can predict the behaviour of a real non-linear system in a working space. Each link is considered as a load system which is connected to the motor. Then, ignoring all non-linear terms in equation (9) it becomes possible to write a simple governing equation for each link

$$\boldsymbol{J}_{\text{eff}}\,\ddot{\theta} + \boldsymbol{C}_{\text{eff}}\dot{\theta} = \tau \tag{10}$$

where $\dot{\theta}$ is the angular velocity, $\ddot{\theta}$ is the acceleration, and τ is the required torque. The non-linear model can be solved using the 'MATLAB Robotic Toolbox' and an equivalent linear plant can be derived for each link as follows

$$\begin{bmatrix}\ddot{\theta} & \dot{\theta}\end{bmatrix} \times \begin{bmatrix} \boldsymbol{J}_{\mathrm{eff}} \\ \boldsymbol{C}_{\mathrm{eff}} \end{bmatrix} = \boldsymbol{\tau} \tag{11}$$

In equation (10), the matrix $[\ddot{\theta}\ \dot{\theta}]$ and vector $\boldsymbol{\tau}$ can be obtained carrying out identifying tests or simulating robot in a defined trajectory. $\boldsymbol{J}_{\mathrm{eff}}$ and $\boldsymbol{C}_{\mathrm{eff}}$ are identifiable terms with respect to defined points in every trajectory. Therefore, for the n points in a trajectory it is possible to write

$$\begin{bmatrix} \ddot{\theta}_0 & \dot{\theta}_0 \\ \ddot{\theta}_1 & \dot{\theta}_1 \\ . & . \\ . & . \\ \ddot{\theta}_n & \dot{\theta}_n \end{bmatrix} \times \begin{bmatrix} \boldsymbol{J}_{\mathrm{eff}} \\ \boldsymbol{C}_{\mathrm{eff}} \end{bmatrix} = \begin{bmatrix} \tau_0 \\ \tau_1 \\ . \\ . \\ \tau_n \end{bmatrix} \tag{12}$$

Suppose,

$$\mathbf{A} = \begin{bmatrix} \ddot{\theta}_0 & \dot{\theta}_0 \\ \ddot{\theta}_1 & \dot{\theta}_1 \\ . & . \\ . & . \\ \ddot{\theta}_n & \dot{\theta}_n \end{bmatrix}, \ \boldsymbol{B} = \begin{bmatrix} \tau_0 \\ \tau_1 \\ . \\ . \\ \tau_n \end{bmatrix} \tag{13}$$

Then,

$$\begin{bmatrix} \boldsymbol{J}_{\mathrm{eff}} \\ \boldsymbol{C}_{\mathrm{eff}} \end{bmatrix} = \mathbf{A}^{\dagger} \times \boldsymbol{B} \tag{14}$$

where,

$$\mathbf{A}^{\dagger} = (\mathbf{A}^{\mathrm{T}}\mathbf{A})^{-1}\mathbf{A}^{\mathrm{T}} \tag{15}$$

For example, equation (9) for the SCARA robot used in [**13**], has the following given numerical values.

$$\mathbf{D} = \begin{bmatrix} 0.538 + 0.237\ \cos\ \theta_2 & -0.192 - 0.118\cos\theta_2 & 0.000 & 0.000 \\ -0.192 - 0.118\cos\theta_2 & 0.195 & 0.000 & 0.085 \\ 0.000 & 0.000 & 1.003 & 0.000 \\ -0.085 & 0.085 & 0.000 & 0.088 \end{bmatrix}$$

$$\boldsymbol{C} = \begin{bmatrix} -\left(\sin\theta_2\left(0.237\dot{\theta}_1\dot{\theta}_2 - 0.118\dot{\theta}_2^2\right)\right) \\ 0.118\dot{\theta}_1^2 \sin\theta_2 \\ 0 \\ 0 \end{bmatrix}$$

$$\boldsymbol{G} = \begin{bmatrix} 0 \\ 0 \\ -9.87 \\ 0 \end{bmatrix} \tag{16}$$

By running the simulation for multiple trajectories for selected known operating points which accurately represent the range of variation in joint dynamics it is found that

$$\text{Link 1} \quad \boldsymbol{C}_{\mathrm{eff}} = [0.75 \quad 5.2], \boldsymbol{J}_{\mathrm{eff}} = [0.2 \quad 0.5] \tag{17}$$

$$\text{Link 2} \quad \boldsymbol{C}_{\mathrm{eff}} = [0.22 \quad 2.12], \boldsymbol{J}_{\mathrm{eff}} = [0.14 \quad 0.26] \tag{18}$$

$$\text{Link 3} \quad \boldsymbol{C}_{\mathrm{eff}} = [0.01 \quad 0.4], \boldsymbol{J}_{\mathrm{eff}} = [0.003 \quad 0.006] \tag{19}$$

$$\text{Link 4} \quad \boldsymbol{C}_{\mathrm{eff}} = [0.52 \quad 0.84], \boldsymbol{J}_{\mathrm{eff}} = [0.15 \quad 0.25] \tag{20}$$

As a result, the linearized transfer function for each link is

$$P_i = \frac{1}{s(\boldsymbol{J}_{\mathrm{eff}}s + \boldsymbol{C}_{\mathrm{eff}})} \qquad i = 1, \ldots, 4 \tag{21}$$

3 APPLICATION OF THE QFT TECHNIQUE TO MULTIPLE-INPUT MULTIPLE-OUTPUT SYSTEMS

Application of the QFT to multiple-input multiple-output (MIMO) uncertain systems is one of the most difficult control problems for engineers. The initial applications of QFT to MIMO systems have been reviewed by Horowitz [**15**] and later developments are discussed in Houpis *et al.* [**16**], D'Azzo and Houpis [**17**], and Horowitz [**18**]. One of the simplest MIMO techniques that can be applied to robot arm manipulators is the one which was introduced by Cheng [**19**]. In this method the basic idea is to convert the closed-loop transfer function to an off-diagonal matrix which can be described as below.

$$\left|\frac{t_{ij}(\mathrm{j}\omega)}{t_{jj}(\mathrm{j}\omega)}\right| \leqslant \lambda_{ij}(\omega) < 1, \quad \text{for} \quad j \neq i \tag{22}$$

where $t_{ij}(\mathrm{j}\omega)$ denotes the relation between jth input to the ith output. Using the fixed point theorem it has been shown that the MIMO system can be represented in terms of equivalent single-input single-output (SISO) systems provided that suitable disturbance rejection bounds are designed. A suitable disturbance rejection model would be the disturbance at the plant output

$$T_{\mathrm{D}} = \frac{1}{1+L} \quad |T_{\mathrm{D}}(\mathrm{j}\omega)| = \left|\frac{Y(\mathrm{j}\omega)}{D(\mathrm{j}\omega)}\right| \leqslant \alpha \tag{23}$$

It was shown in [**19**] that in order to achieve an off-diagonal closed-loop transfer function the following inequality must hold

$$\left|\frac{1}{1+l_i(\mathrm{j}\omega)}\right| \leqslant \min\left(\frac{\sigma_{ij}(\omega)}{|q_{ii}(\mathrm{j}\omega)/q_{ij}(\mathrm{j}\omega)|_{\max}}\right. \\ \left.\text{for} \quad i \neq j, \quad j = 1, 2, \ldots, n\right), \quad \omega \leqslant \omega_h \tag{24}$$

where l_i is the open-loop transfer function, $[1/q_{ij}] = P^{-1}$, and σ_{ij} is a small positive function which bounds the closed-loop transfer function. Therefore, based on this inequality and the iteration algorithm described in [**19**] it is possible to design suitable disturbance rejection bounds.

4 QFT CONTROLLER DESIGN

This section uses the QFT method [**14**, **20**] to design a controller for a SCARA robot. The non-linear plant needs to be converted to family of linear and uncertain processes and the techniques introduced in section 2 need to be implemented. The objectives of this section are to synthesize suitable controllers and prefilters such that:

(a) the closed-loop system is stable;
(b) it can track desired inputs;
(c) cross-coupling effects can be studied by using suitable robust disturbance rejection bounds.

The stability margin can be defined by

$$\left|\frac{P(\mathrm{j}\omega)G(\mathrm{j}\omega)}{1+P(\mathrm{j}\omega)G(\mathrm{j}\omega)}\right| < 1.2$$

The tracking specification is an overshoot of 20 per cent and a settling time of 0.08 s for all plant uncertainties which can be described with the second-order system

$$|\alpha(\mathrm{j}\omega_i)| \leqslant |T(\mathrm{j}\omega_i)| \leqslant |\beta(\mathrm{j}\omega_i)|$$

where $\alpha(\mathrm{j}\omega_i)$ and $\beta(\mathrm{j}\omega_i)$ are lower bound and upper bound respectively. $T(\mathrm{j}\omega_i)$ is the input–output relation from the input $R(s)$ to the output $Y(s)$.

Suitable robust disturbance rejection bounds to reduce the cross-coupling effects between joints are

$$\left|\frac{1}{1+l_i(\mathrm{j}\omega)}\right| \leqslant \lambda(\omega)$$

For a dynamic model of the SCARA the main cross-coupling effects are between the first and second links, thus a MIMO control approach is used for the first and second joints and a SISO control approach for the third and fourth joints. Table 1 shows $\lambda(\omega)$ for first and second links over the design frequencies.

As a first step the plant uncertainty (template) must be defined and the computed boundary of plant templates for link 1 are shown in Fig. 5. The robust margin bounds are depicted in Fig. 6 and the robust disturbance rejection and robust tracking bounds are shown in Figs 7 and 8 respectively. Finally, the intersection of bounds or the robust performance bound is shown in Fig. 9.

The loop shaping and pre-filter functions were calculated the QFT toolbox in MATLAB. The results

Table 1 Robust disturbance rejection bounds

	ω_i						
	10	30	50	80	100	140	500
Link 1	0.1002	0.171	0.298	0.387	0.5890	0.88	0.92
Link 2	0.113	0.143	0.218	0.3613	0.5036	0.77	0.82

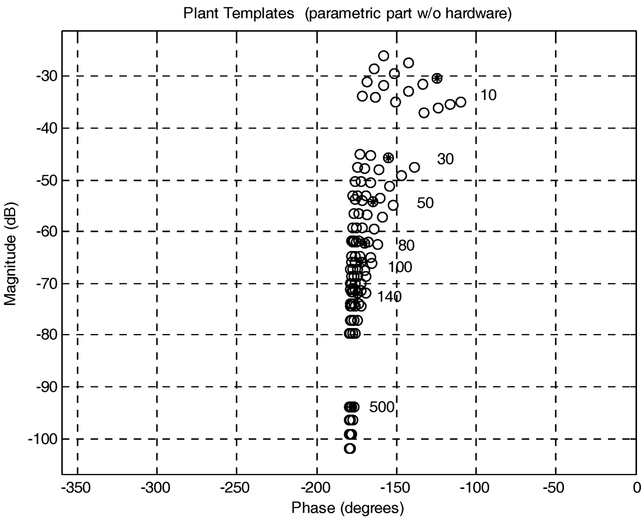

Fig. 5 The boundary of the plant template for link 1

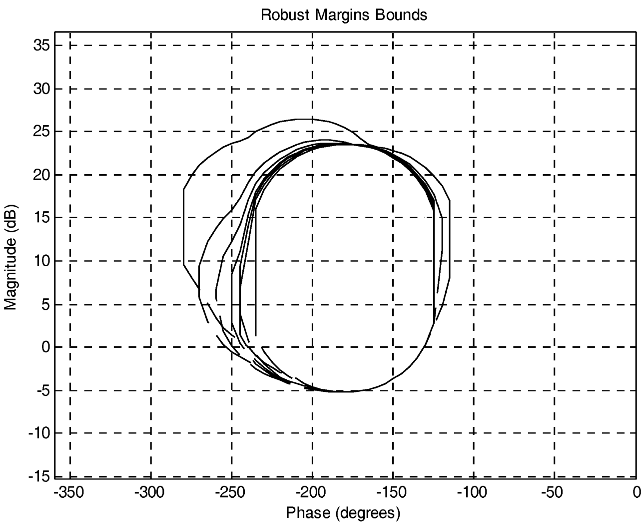

Fig. 6 Robust margin for link 1

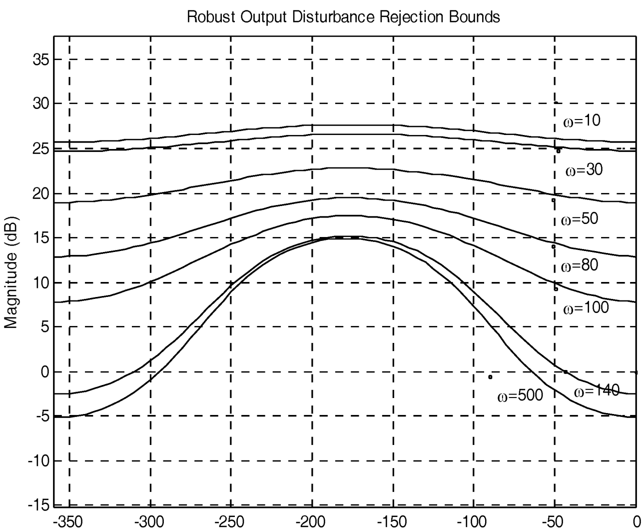

Fig. 7 Robust disturbance rejection bounds for link 1

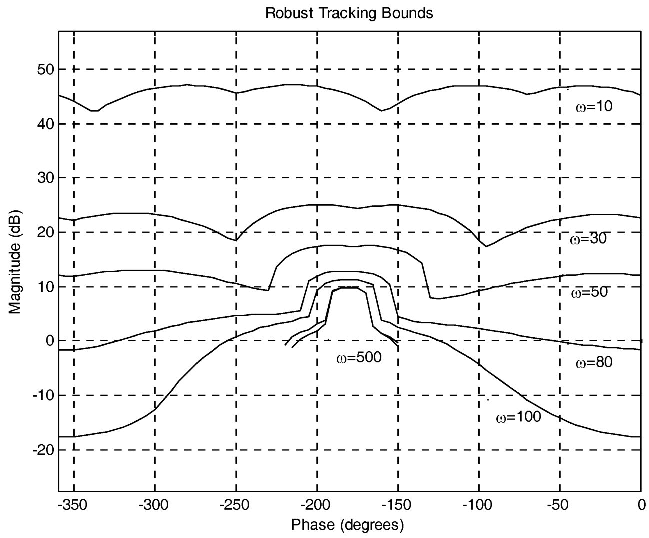

Fig. 8 Robust tracking bounds for link 1

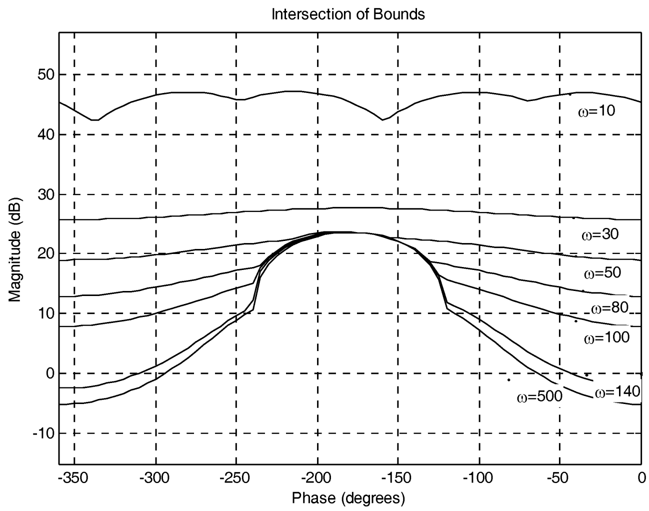

Fig. 9 Intersection of bounds for link 1

are presented in Figs 10 and 11 respectively [**14**]. In order to save the space, only the controller design process is shown for the first link in this paper.

The related controllers for each link are found to be

$$G_1(s) = 4337\,\frac{(1+s/5.213)(1+s/52.98)}{(1+s/12.26)(1+s/432)} \tag{25}$$

$$G_2(s) = 330.5\,\frac{(1+s/12.61)(1+s/132.4)}{(1+s/77.88)(1+s/326.9)} \tag{26}$$

$$G_3(s) = 770.1\,\frac{(1+s/4.04)(1+s/75.93)}{s(1+s/1089)} \tag{27}$$

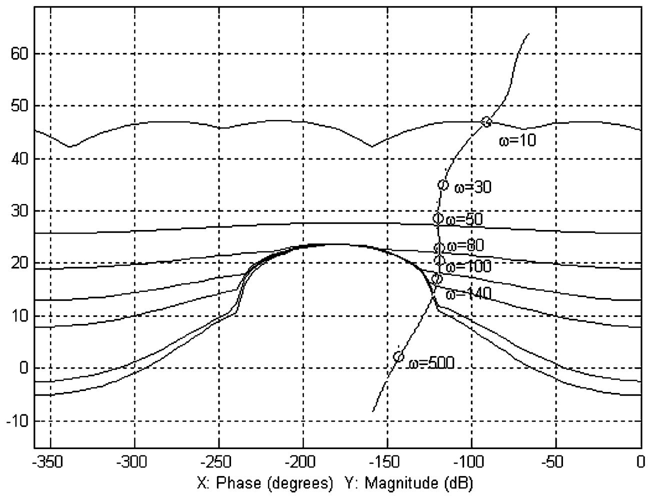

Fig. 10 Loop-shaping in Nichols' chart for link 1

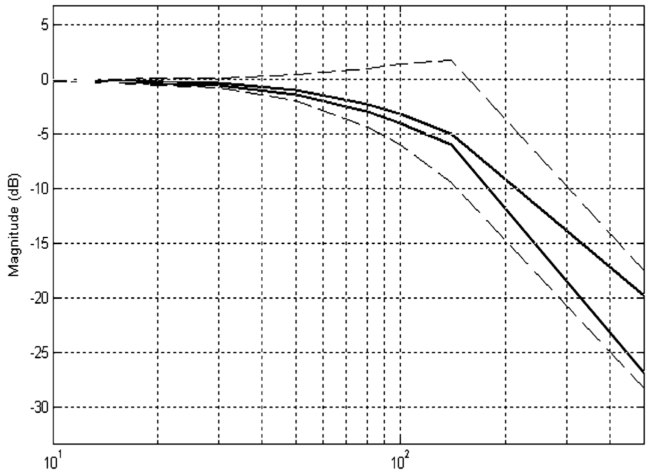

Fig. 11 Pre-filter shaping for link 1

$$G_4(s) = 6480\,\frac{(1+s/2.351)(1+s/48.37)}{s(1+s/1302)} \tag{28}$$

The related pre-filters for the robot links are

$$F_1(s) = \frac{1}{(1+s/70)} \tag{29}$$

$$F_2(s) = \frac{1}{(1+s/62)} \tag{30}$$

$$F_3(s) = \frac{(1+s/130)}{(1+s/73.4)(1+s/126.1)} \tag{31}$$

$$F_4(s) = \frac{1}{(1+s/60)} \tag{32}$$

The robust stability is shown in Fig. 12 and Fig. 13 shows the time-domain closed-loop response

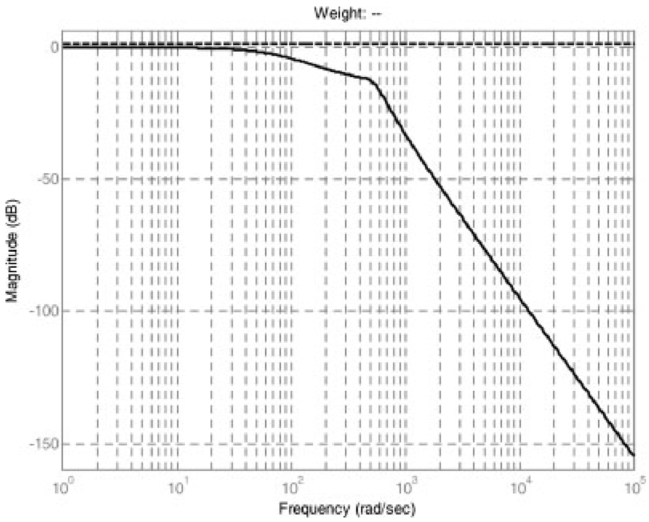

Fig. 12 Robust stability in the frequency domain for link 1

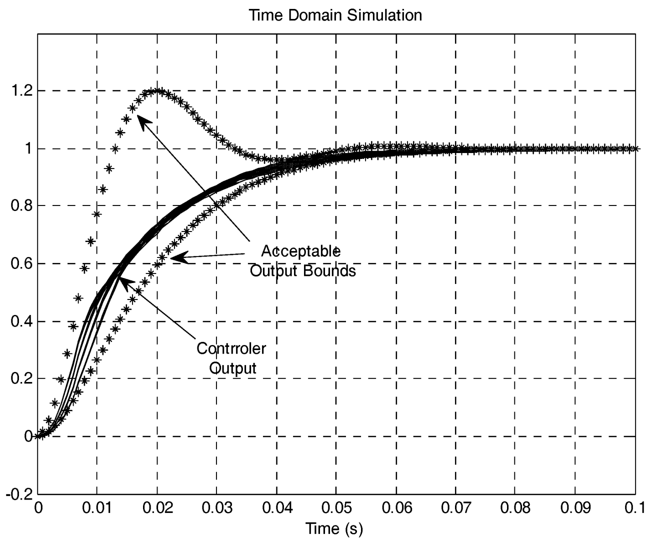

Fig. 13 Time-domain simulation for link 1, considering all of the system uncertainty

of the associated linear system for the robots' dynamics.

According to the linear simulation the robot has robust stability and can also satisfy tracking specifications. However, the main objective in applying QFT to non-linear systems is to get satisfactory results through non-linear simulations. Thus, in the next section non-linear simulation will be performed.

5 SIMULATION RESULTS AND DISCUSSION

In this section non-linear simulations will be performed using the control strategy shown in

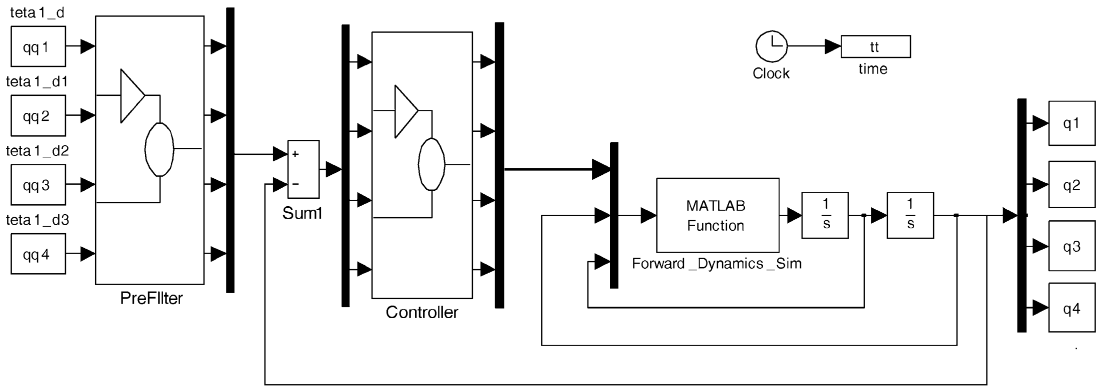

Fig. 14 Block diagram of the control strategy

Fig. 14. The robustness of the proposed design in tracking problems is tested by moving the robot in a three-dimensional (3D) elliptical path. The results obtained for the tracking problem are shown in Fig. 15 and the associated tracking error is shown in Fig. 16. The tracking error for the same path, but using a SISO control approach is shown in Fig. 17. It can be seen that the robust QFT controller demonstrates excellent robustness properties and tracking ability, and the comparison of the MIMO and SISO approaches indicates the effectiveness of the MIMO approach.

6 CONCLUSIONS

The presence of uncertainty in the dynamics of robot arm manipulators means that the application of robust control methods to achieve a high accuracy in tracking is inevitable. QFT has been used to design a robust controller for a SCARA robot. The basic design steps can be summarized as the linearization of the robot dynamics, the design of suitable robust disturbance rejection bounds by minimization of a sensitivity function, linear simulation, and non-linear simulation. The presented results show that the increase in the accuracy achieved for the tracking problem is a direct result of the reduction of the cross-coupling effect between joints created by designing suitable disturbance rejection bounds, the reduction of settling time in tracking bounds for associated linear system, and improvement of associated linear uncertain system modelling. Non-linear simulation of the tracking of a 3D elliptical path indicates that the QFT controller has a consistent tracking ability, and also application of the MIMO control approach will greatly improve the

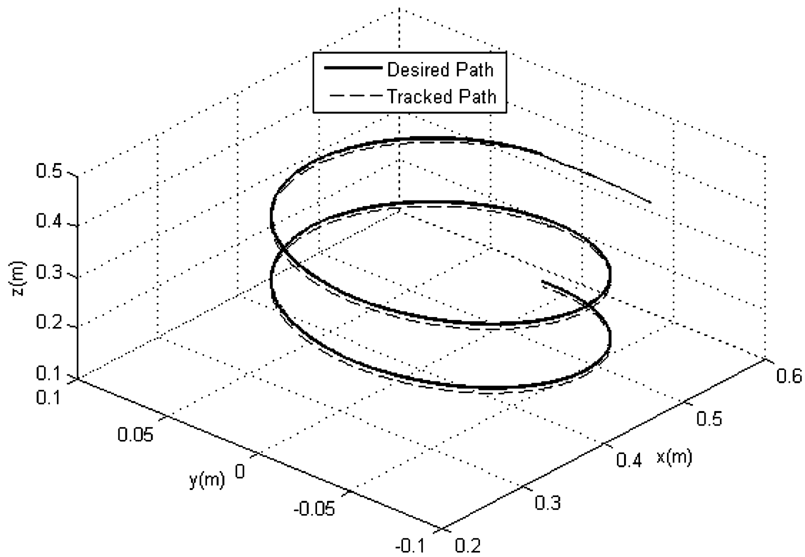

Fig. 15 Tracking problem for a 3D elliptical path

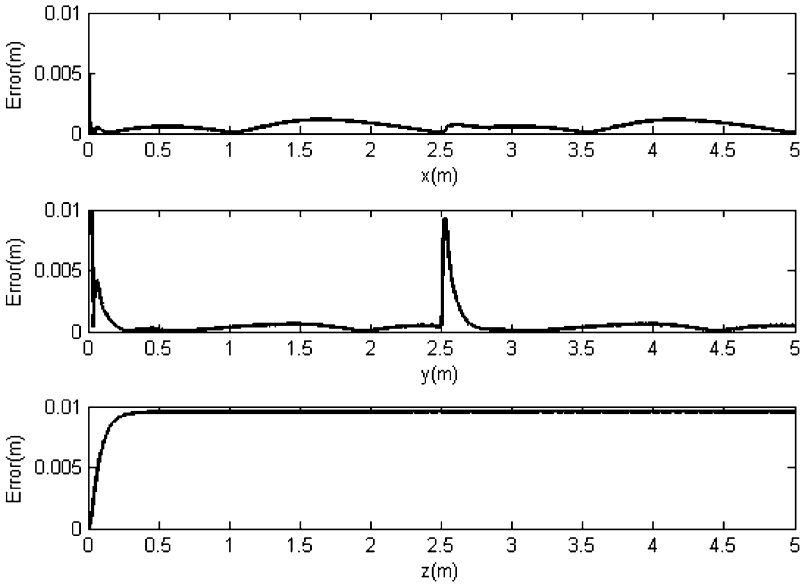

Fig. 16 End effecter error in Cartesian coordinate system based on the MIMO approach

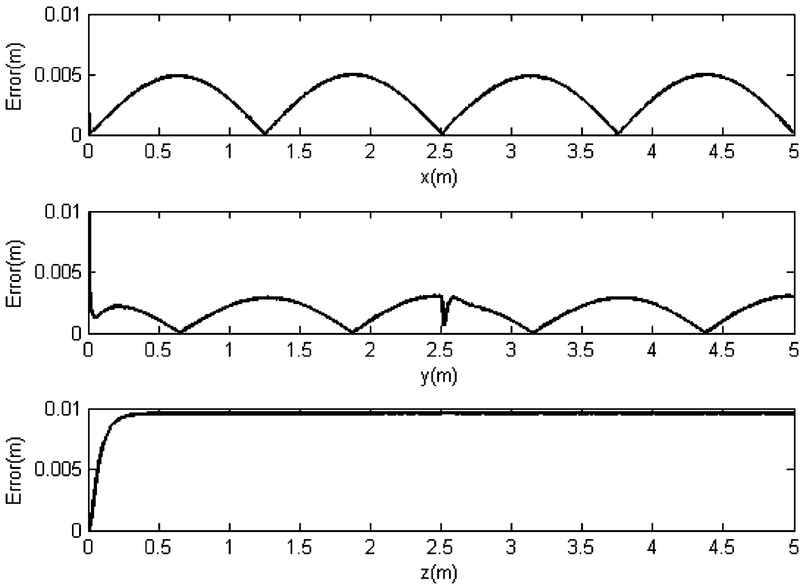

Fig. 17 End effecter error in Cartesian coordinate system based on the SISO approach

performance of the system compared to the SISO control approach.

REFERENCES

1 **Meng, E.** and **Liew, K.** Control of adept one SCARA robot using neural networks. *IEEE Trans. Ind. Electron.*, 1997, **44**, 762–768.

2 **Kang, Z. B., Chai, T. Y., Oshima, K., Yang, J. M.,** and **Fujii, S.** Robust vibration control of SCARA-type robot manipulators. *Control Engng Practice*, 1997, **5**(7), 907–917.

3 **Tern, T. J., Bejeay, A. K., Lotdorl, A.,** and **Chen, Y.** Nonlinear feedback in robust link control. In Proceedings of the IEEE *Control conference*, New York, 1984, pp. 38–51 (IEEE, Piscataway, New Jersey).

4 **Horowitz, I. M.** and **Sidi, M.** Synthesis of feedback systems with large plant ignorance for prescribed time domain tolerances. *Int. J. Control*, 1972, **16**, 287–309.

5 **Horowitz, I. M.** and **Sidi, M.** Optimum synthesis of nonminimum phase feedback system with plant uncertainty. *Int. J. Control*, 1978, **27**, 361–386.

6 **Horowitz, I. M.** *Quantitative Feedback Design Theory (QFT), volume 1*, 1993 (QFT Publications, Boulder, Colorado).

7 **Houpis, C. H.** Quantitative feedback theory (QFT) for the engineer: a paradigm for the design of

control systems for uncertain nonlinear plants. Wright Patterson Air Force Base, 1995.

8 **Yaniv, O.** *Quantitative feedback design of linear and non-linear control* systems, 1998 (Kluwer Academic Publishers, Norwell, Massachussets).

9 **Asnaashari, M. S.** *Design and product of a software for simulating behavior of robot manipulators in inverse kinamatics and control problems by classic and neuro-fuzzy methods*. M Science Thesis, 2005, Department of Electrical Engineering, Ferdowsi University of Mashhad, Iran.

10 **Luh, J. Y. S.** An anatomy of industrial robots and their controls. *IEEE Trans. Autom. Control*, 1983, **28**(2), 133–153.

11 **Lewis, F. L., Stevens Jr, G. T., Zhou, C.,** and **Priest, J. W.** *Robotics*, 1999 (CRC Press, Boca Raton, Florida).

12 **Niksefat, N.** and **Sepehri, N.** Robust force controller design for an electrohydraulic actuator based on nonlinear model. In Proceedings of the IEEE Conference on *Robotics and automation*, Detroit, MI, 10–15 May 1999, pp. 200–206 (IEEE, Piscataway, New Jersey).

13 **Taghirad, H.** and **Afshar, S.** Design of PID controller for linear SCARA. In Proceedings of the 8th International Conference on Electrical Engineering, Isfahan, May 1999, pp. 161–168.

14 **Gharib, M., Amiri Moghadam, A. A.,** and **Moavenian, M.** Robot technology and applications. International Symposium on Automation and Robotics in Construction (ISARC), Kochi, Kerala, India 19–21 September 2007.

15 **Horowitz, I.** Survey of quantitative feedback theory (QFT). *Int. J. Control*, 1991, **53**, 255–291.

16 **Houpis, C. H., Rasmussen, S. J.,** and **Garcia-Sanz, M.** *Quantitative feedback theory, fundamentals and applications,* second edition, 2005 (Marcel Dekker, New York).

17 **D'Azzo, J. J.** and **Houpis, C. H.** *Linear control systems*, 1995, pp. 580–737 (McGraw-Hill, New York).

18 **Horowitz, I.** *Quantitative feedback theory (QFT), volume 1*, 1993 (QFT Publications, Boulder, Colorado).

19 **Cheng, C.-C., Liao, Y.-K.,** and **Wang, T.-S.** Quantitative feedback design of uncertain multivariable control systems. *Int. J. Control*, 1996, **65**(3), 537–553.

20 **Nataraj, P. S. V.** Computation of QFT bounds for robust tracking specifications. *Automatica*, 2002, **38**, 327–334.